Classical Polarization in Hybrid QM/MM Methods

Christopher J. R. Illingworth,[†] Stuart R. Gooding,[†] Peter J. Winn,[†,‡] Garth A. Jones,[†] György G. Ferenczy,[§] and Christopher A. Reynolds*[,†]

Department of Biological Sciences, University of Essex, Wivenhoe Park, Colchester, CO4 3SQ, United Kingdom, and Department of General and Analytical Chemistry, Budapest University of Technology and Economics, Szt Gellért tér 4, Budapest, 1111-Hungary

Received: July 10, 2004; In Final Form: March 29, 2006

We have presented a method for modeling polarization in hybrid QM/MM calculations. The method, which expresses the induced dipoles as a set of "induced" charges, is based on the induced dipole approach and methodology for calculating potential-derived point charges from distributed multipole series. The method has the advantage that the same methodology can be used to determine the induced charges and the potential derived charges and so both sets of charges are rigorously defined within the same framework. This underlying link with the wave function makes the method particularly suitable for use in hybrid QM/MM calculations. Here we assess the importance of explicit polarization in the classical part of a QM/MM system with regard to improving the classical description and the consequent effects on the quantum description. The main advantages of the induced charge approach are that the method is readily interfaced with quantum mechanical methods and that induced charges are more readily interpreted than induced dipoles. The ease of interpretation is illustrated by analysis of the charges involved in dimeric and trimeric hydrogen bonded systems. The method for treating the MM polarization has been validated by a regression analysis of the charges induced in both the QM and MM systems against those derived from full quantum mechanical calculations. The method has also been validated using two energy decomposition approaches, which show that MM polarization makes a significant and reliable contribution to the QM − MM interaction energy in a hybrid system. The distance dependency of the induced charges is investigated in calculations on methylsuccinyl-Ala-Ala-Pro-Ala chlormethyl ketone interacting with human neutrophil elastase and propranolol interacting with asparagine residues in a model of the β_2-adrenergic receptor.

Introduction

Hybrid quantum mechanics molecular mechanics (QM/MM) methods[1−3] offer much potential in modeling, particularly because they offer a strategy for calculating the energetics of an enzyme catalyzed reaction.[4−18] They also offer a parameter-free approach for studying both the conformation and the polarization of a quantum mechanical ligand within a classical enzyme. In some cases, the polarization has been shown to play a key part in priming substrates for reaction.[9,19,20] Such effects cannot normally be observed with current molecular mechanics force fields that are in widespread routine use (e.g., AMBER,[21−24] OPLS,[25−28] CHARMM[29−31]) as polarization is usually included implicitly rather than explicitly. Moreover, the advantages of hybrid QM/MM methods are not restricted to enzyme reactions but can also be applied to inorganic systems such as transition metal complexes.[32−34] Here we describe a method for explicitly including polarization in classical force fields that can be readily interfaced with quantum mechanical methods. It is allied to the method of deriving atomic charges (monopoles) from the quantum mechanical electrostatic potential[35] and is therefore compatible with many of the force fields in current use.[22,36] We assess the importance of polarization of the classical part of a QM/MM system both from the perspective of better representing the classical part and from the perspective of its influence on the quantum part.

Stone has presented a rigorous theory for describing polarization[37] that gives excellent results on small molecules[38,39] but, the method is not readily applicable to large biomolecular systems. For such systems, the usual simplification is to assign point charges, q, and isotropic scalar polarizabilities, α, to the atoms; here, as elsewhere,[40,41] we used the isotropic atomic polarizabilities of Miller and Savchik.[42] The field, **E**, due to the point charges, q (and the induced dipoles, μ), then gives rise to induced dipoles, μ, via

$$\mu = \alpha \mathbf{E} \tag{1}$$

The induced dipoles, μ, modify the field, **E**, and so eq 1 is usually solved by iteration, but considerable improvement in accuracy can still be obtained without iteration[43−45] and hence with consequent savings in CPU time. The dipole, μ, and the field, **E**, are shown in bold to denote that these are vector quantities: this increase in complexity inevitably adds a high computational overhead to the calculations and also makes them more difficult to interpret. Nevertheless, the method has been applied to a number of systems, notably water.[46−51] Kollman and Hemmingsen have shown that polarization may be essential for describing the hydration of cations.[52,53] A number of authors have shown that the polarization energy is particularly significant in condensed phases and typically constitutes 10−20% of the total interaction energies.[43,54−59]

* Corresponding author. E-mail: C.A.Reynolds@essex.ac.uk.
† University of Essex.
‡ Current address: European EML Research gGMbH, Villa Bosch, Schloss-Wolfsbrunnenweg 31c, 69118 Heidelberg, Germany.
§ Budapest University of Technology and Economics.

10.1021/jp046944i CCC: $33.50
Published on Web 05/03/2006

TABLE 1: Comparison of B3LYP/DZVP Potential-Derived Charges,[83] Mulfit Charges[59] and Mulliken Charges[109] for the Pathological Case of $[Zn(H_2O)_6]_2^+$ [a]

	q(MEP)	*q*(Mulfit)	*q*(Mulliken)
Zn	9.236	−0.012	1.082
O	−2.178	−0.768	−0.361
H	0.486	0.385	0.257

[a] The molecular electrostatic potential (MEP)-derived charge method fails on the buried Zn atom.

Approaches to polarization based on fluctuating charges, the related chemical potential equalization model and the Drude oscillator model[60−67] offer much potential for studying biomolecular systems because the polarization is handled at the point charge level and so the computational overhead is small;[63] work for including these methods in hybrid QM/MM methods is underway.[68−70]

We have followed an alternative approach to polarization. Previous methods for calculating potential-derived point charges[59,71,72] from a distributed multipole analysis (DMA)[73,74] are used to express the induced dipole, derived from eq 1, as a set of "induced" charges on the atom carrying the isotropic polarizability, α, and those bonded to it. The method has the advantage that the same methodology is used to determine the induced charges and the potential derived charges and so both sets of charges are rigorously defined within the same framework. The link with the wave function is therefore retained and this offers both compatibility with hybrid QM/MM methods and the option to derive charges (and other parameters) unambiguously from the wave function. This point is important because many force fields are parametrized against total energies without a rigorous attempt to meaningfully separate the energy components. The method has been implemented in a fully classical framework[41] and an application of the method to the iodine−oxygen nonbonded interaction in dimethyl-2-iodobenzoylphosphonate has been reported.[40] Here we present a more complete report of the ability of the hybrid QM/MM method to reproduce the electronic distributions in the classical and quantum components of a number of small hybrid QM/MM systems, and introduce some of the issues that may be relevant for calculations on large systems.

Methods

The systems chosen consist of a number of dimeric or trimeric nonbonded complexes that were sufficiently small to be studied using full quantum mechanical calculations. The B3LYP density functional method[75] was used to determine the energies and optimized geometries, primarily because charge distributions derived from density functional wave functions do not include polarization implicitly[59] but also because the B3LYP method can give a good description of hydrogen bonding,[76,77] as long as dispersion effects are not important.[78] A relatively large TZVP basis set of triple-ζ plus polarization quality designed for density functional calculations[79,80] was used because of its compatibility with density functional calculations and because its large size should help to minimize basis set superposition effects,[81] which were estimated using the counterpoise correction.[82] (For the zinc complex, $[Zn(H_2O)_6]^{2+}$ (Table 1), a related DZVP basis set[79,80] was used because the TZVP basis set is not available for zinc; the DZVP basis set was also used for the large protease ligand). Symmetry was not rigorously applied, because it is rarely useful in biology, and so some charges may differ slightly even though they appear to be in identical environments. The charges were determined using the mulfit methodology.[59,71,72] These are essentially potential derived charges in which the potential is determined from a distributed multipole analysis up to hexadecapole in a spherical shell around the multipole center. The optimal charges that reproduce this potential on the multipole center and the atoms bonded to it are determined using an analytical procedure that avoids the use of a numerical grid. Because the atomic charges are linked to the multipole expansion on the same atomic center (and those bonded to it), the method does not suffer problems with ill-defined charges as may occur with other implementations of the potential-derived charge method.[36,83−86] A catastrophic failure of the standard potential-derived charge method is shown for $[Zn(H_2O)_6]^{2+}$ in Table 1. Here the potential was calculated from the distributed multipole expansion of the GAUSSIAN[87] wave function using ORIENT[88] at a surface of 955 randomly distributed points on a surface at twice the van der Waals radius. Such failures depend on the surface chosen and arise partly because atoms distant from a center contribute toward the potential in its vicinity and these failures are most noticeable for buried atoms such as the Zn in Table 1: there are several such atoms in this study. We note that the RESP and related charge fitting procedures[86,89,90] also avoid unrealistically high values for charges but require extra constraints, unlike the methodology described here.

For each system in this study, one of the molecules was described quantum mechanically and the remainder described classically. The polarized wave function and the induced charges on the classical atoms were calculated iteratively. First, the monomer charges were assigned on the classical (MM) molecule and these charges were used as a perturbation in the Hamiltonian to polarize the quantum mechanical (QM) entity.[91−95] The classical molecules were polarized via eq 1, with the electric field at the MM atoms due to the QM entity potentially calculated by one of two methods. The first is calculation of the field directly from the wave function using GAUSSIAN.[87] In the second, the wave function was calculated using GAUSSIAN and expressed as a distributed multipole analysis using GDMA 1.3.[96] The field was then calculated from this multipole series using ORIENT 4.5.[88] For both of these approaches, the induced dipoles on the MM entity were calculated using eq 1 and expressed as induced charges using the mulfit technology described above.[40,41,59,71,72] Both methods gave essentially equivalent results but the second method was quicker and was used for all the results reported here. The induced charges were added to the monomer charges and the new charges replaced the original charges as the perturbation to the Hamiltonian. This resulted in a new wave function, new fields and new induced charges. The procedure was iterated (typically for 4 iterations) until the value of the induced charges converged. As implemented here, the method does not readily permit the calculation of analytical gradients, but this limitation has been removed in a related method[43] that uses an alternative approach for converting induced dipoles into induced charges and is therefore more suited to geometry optimization and molecular dynamics.

To avoid the "polarization catastrophe", we followed the procedure of not allowing atoms separated by 3 bonds or less to polarize each other. A less obvious problem, which can be corrected for, is the corruption of the monomer charges by the polarizing effect of atoms in the same monomer unit.[41] Here this was not a major problem and was ignored.

For the trimeric systems, two approaches to the polarization were employed. In the first, only the field from the QM entity was used in the calculations. In the second, the two MM entities were also allowed to polarize each other; here the field at MM

entity 1 due to the QM entity was augmented by the classical field (again calculated using ORIENT) due to MM entity 2 (and vice versa).

A simple energy decomposition scheme[91,92] was applied to the fully optimized complexes to determine the quantum mechanical electrostatic and polarization energy so that the energetic contribution of MM polarization to the polarization of the QM entity within the hybrid system could be assessed. Let E_1 be the quantum mechanical energy of the isolated monomer and let its wave function be used as the guess for the wave function in the hybrid QM/MM calculation. Let E_2 be the energy at the end of the first SCF cycle and E_3 the energy when the SCF process has converged. The monomer charges are then incremented by the induced charges and used in the Hamiltonian and E_4 is the energy at the end of the SCF process when this wave function has converged (i.e., after the first iteration). E_5 is the corresponding energy at the end of the SCF process after 4 iterations. Under these circumstances, $E_2 - E_1$ is the electrostatic energy and $E_3 - E_2$ is the SCF polarization energy. Taken with the self-energy correction (see below), $E_4 - E_3$ gives the MM polarization energy after 1 iteration and $E_5 - E_4$ gives the additional MM polarization energy after the iteration has converged (i.e. after 4 cycles). In all cases, iteration refers to iteration of the induced charges and not to SCF cycles.

The self-energy, E_{self}, is the energy required to create the induced charges. Ferenczy and Reynolds[43] give two alternative ways for calculating this correction within a purely classical framework.

$$E_{self} = \frac{1}{2}\sum_{ij}\frac{1}{r_{ij}}q_i^{ind}q_j^{tot} \tag{2a}$$

$$E_{self} = \frac{1}{2}\sum_{i}^{atoms}\alpha_i E_i^2 \tag{2b}$$

Here the more common method of calculating E_{self} from the electric field, E_i, and polarizabilities, α_i at the MM atoms i, (2b), overestimates the correction as it assumes isotropic polarization and so here we used the QM/MM analogue of eq (2a) which, as in equations (2a) and (2b), gives the MM polarization energy as half the total polarization energy calculated in the absence of the self-energy calculation.

Morokuma energy decomposition analysis,[97] implemented at the Hartree−Fock level within GAMESS-US[98] was used to determine the polarization component of the total quantum mechanical interaction energy. This program partitions the energy into an electrostatic, polarization, charge-transfer, exchange repulsion and a contribution (termed "mix") that cannot be assigned to any of the other categories. The "mix" term was added to the counterpoise correction to give an upper limit to the error in the polarization component. The Morokuma energy decomposition analysis does not give a unique partitioning but it does provide a useful independent benchmark against which the QM/MM calculations can be assessed. For this reason, some of the QM/MM calculations were also performed at the Hartree−Fock level using the same TZVP basis set, or the 6-31G* basis set[99] for the propranolol-β_2-adrenergic receptor system, because this basis set or a similar one is usually used for such applications in biology).

The statistical analysis was performed using SPSS 11.5;[100] in all determinations of F and t the probability that the results arose by chance was given as 0.000 and so is not reported below.

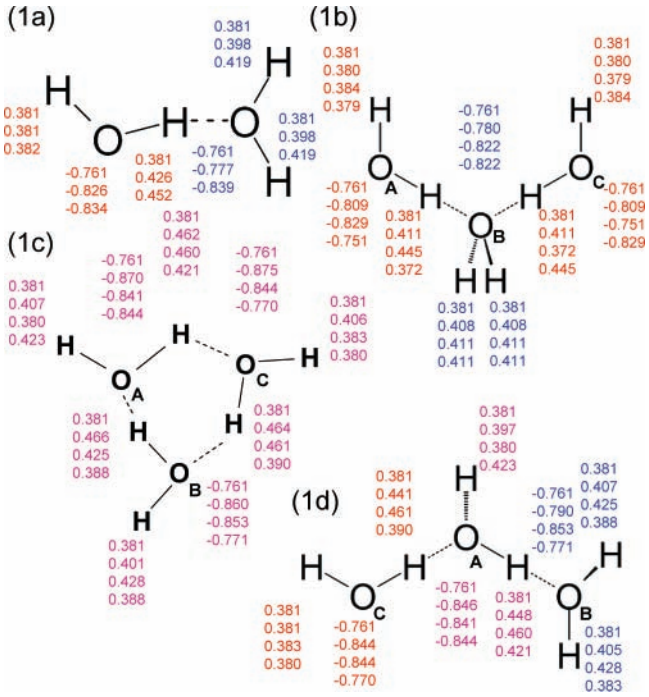

Figure 1. Atomic charges for (a) the water dimer, (b) the anticooperative water trimer, (c) the cyclic water trimer and (d) the linear cooperative water trimer. The order of the charges from top to bottom is (i) QM monomer charge, (ii) full QM complex charge, (iii) MM polarized charge 1, (iv) (trimers only) MM polarized charge 2 (i.e., with the alternative monomer as the QM entity. The order of the classical charges (iii) and (iv) is ABC, so if C is the molecule under focus, the order of the MM charges is for A as QM followed by B as QM; the molecules are labeled by a subscript on the oxygen atom.). The charges did not include the classical correction (as is apparent from the disparity at some positions between (iii) and (iv)) and were obtained after one iteration.

Results and Discussion

Qualitative Analysis of the Induced Charges. The results are readily illustrated by calculations on water dimers and trimers, as shown in Figure 1. The anticooperative water trimer (1b) shows the least increase in polarity, followed by the dimer (1a), the linear cooperative trimer (1d) and last the cyclic water trimer (1c). The results for the full set of the additional molecules (Figure 2 plus the A-T and A-U base pairs) are given in Figures S1−5S. These charges are the simplest that can be calculated under the schemes presented here as they were calculated after 1 iteration and did not include the classical correction to the field. The systems studied here interact through hydrogen bonds and so the qualitative power of the method can be seen by analyzing the charges on the oxygen and nitrogen atoms that (a) donate hydrogen bonds (Table 2), (b) receive hydrogen bonds (Table 3) and (c) donate and receive hydrogen bonds (Table 4). Table 5 shows that the charges usually converged after 3 cycles of iteration, particularly for atoms not involved in hydrogen bonding. Indeed, the rapid convergence for many atoms suggests strategies for reducing the computational effort that will be investigated further below. Initially, however, in Tables 2−4, we concentrate on the charges determined after full iteration with the classical correction to the field.

Some of the systems presented below display quite subtle effects that arise because of the interplay between different hydrogen bonds. For example, in the water trimer in Figure 1b, the outer water molecules polarize the central molecule via the same oxygen atom. Vectors drawn from the central oxygen to the hydrogen-bonding hydrogen atoms of the flanking water

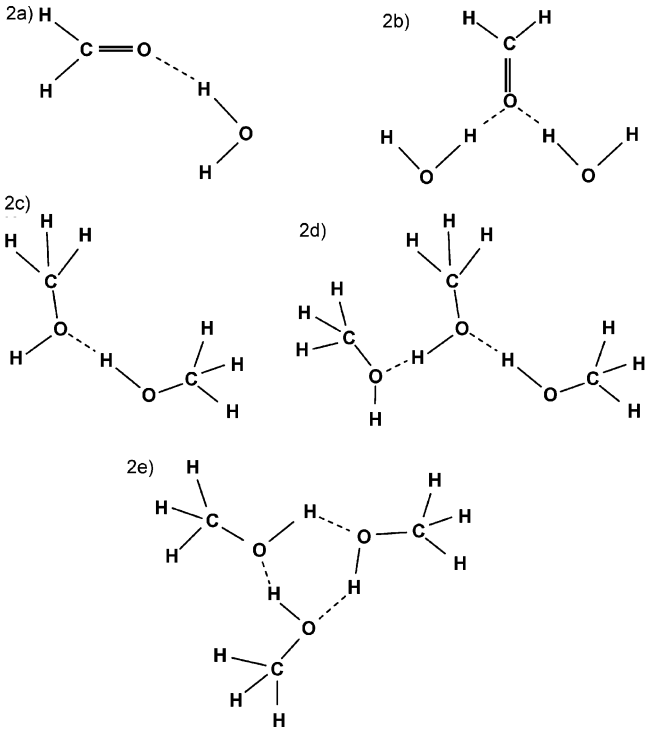

Figure 2. Additional molecules under study; the A-T and A-U base pairs were also studied in addition to the oligomers shown here.

TABLE 2: B3LYP Atomic Charges on Hydrogen Bond Donating Heavy Atoms[a]

atom	monomer charge	quantum charge	induced charge	system
O	−0.76	−0.81	−0.79	water formaldehyde anticooperative trimer
O	−0.76	−0.80	−0.81	water formaldehyde dimer
O	−0.76	−0.83	−0.83	water dimer
O	−0.76	−0.81	−0.81	anticooperative water trimer
O	−0.76	−0.84	−0.85	cooperative water trimer
O	−0.66	−0.70	−0.74	methanol dimer
O	−0.66	−0.72	−0.75	linear methanol trimer
N	−0.49	−0.55	−0.56	N3 of T on AT
N	−0.50	−0.55	−0.57	N3 of U on AU
N	−0.53	−0.58	−0.58	N^6 of A in AT (or AU)

[a] For the trimer systems, the induced charge calculations incorporated the classical correction. The charges reported are those obtained after four cycles of iteration but are generally the same at 2dp as those obtained after 1 iteration. For the trimer systems, as there are three ways to select the monomer to be treated quantum mechanically, it is possible to report two induced charges for each atom, one for each QM monomer. However, with the classical correction (but not without), these values are largely the same at 2dp and so the common value is reported in Tables 2−4. However, in a few cases where there are multiple equivalent values, e.g., FWW, a consensus is reported (but in Table 6 all values are used).

molecules are essentially opposed to each other. In some respects, therefore, the hydrogen bonds are working against each other and the hydrogen bond system is termed anticooperative. In contrast, in (1d), the corresponding oxygen to hydrogen vectors point in the same direction. In this system, (1d), the hydrogen bonds re-enforce each other and the hydrogen bond system is cooperative. These effects are magnified in the cyclic cooperative systems in Figures 1c and 2e. Similar effects work to re-enforce the two A-T and A-U hydrogen bonds in the base pairs (Figure S5, Supporting Information).

Hydrogen Bond Donating Heavy Atoms. Table 2 shows that for the water oligomers, the anticooperative trimer generally has the smallest increase in polarity (as shown by the quantum charges), followed by the dimer and then the cooperative trimer. This effect is well reproduced by the induced charges. A similar increase in polarity in the methanol trimer over the dimer is again well reproduced. The ability of formaldehyde to polarize a water molecule is generally less than that of another water molecule and this is reflected well in the changes in the induced charges. The change in polarity in the anticooperative formaldehyde water heterotrimer compared to the dimer is minimal because the polarizing power of the formaldehyde is split between the two water molecules. For the base pairs, the increase of ∼−0.05 in charge on N^6 and N3 of A and T (or U) is well reproduced.

TABLE 3: B3LYP Atomic Charges on Hydrogen Bond Accepting Heavy Atoms[a]

atom	monomer charge	quantum charge	induced charge	system
O	−0.51	−0.55	−0.56	water formaldehyde anticooperative trimer
O	−0.51	−0.53	−0.54	water formaldehyde dimer
O	−0.76	−0.78	−0.84	water dimer
O	−0.76	−0.78	−0.88	anticooperative water trimer
O	−0.76	−0.79	−0.86	cooperative water trimer
O	−0.66	−0.66	−0.70	methanol dimer
O	−0.66	−0.68	−0.71	linear methanol trimer
O	−0.61	−0.67	−0.66	O^4 of T
O	−0.60	−0.67	−0.65	O^4 of U
N	−0.70	−0.77	−0.78	N1 on A in AT
N	−0.70	−0.79	−0.78	N1 on A in AU

[a] The other details are as for Table 2.

TABLE 4: B3LYP Atomic Charges on Heavy Atoms that Donate and Accept Hydrogen Bonds[a]

atom	monomer charge	quantum charge	induced charge	system
O	−0.76	−0.85	−0.92	cooperative water trimer
O	−0.76	−0.87	−0.90	cyclic cooperative water trimer
O	−0.66	−0.72	−0.76	linear methanol trimer
N	−0.66	−0.73	−0.76	cyclic methanol trimer

[a] The other details are as for Table 2.

TABLE 5: Variation in Charge with Iteration for Atoms of the Water Dimer[a]

atoms	monomer	first	second	third	fourth	fifth
			Left Water of Water Dimer			
O	−0.761345	**−0.83**3582	**−0.8348**66	**−0.83489**0	**−0.834891**	**−0.834891**
H	0.380775	**0.381**739	**0.381664**	0.381663	**0.381663**	**0.381663**
H	0.380680	**0.45**1842	**0.4532**01	**0.45322**7	**0.453228**	**0.453228**
			Right Water of Water Dimer			
O	−0.761345	**−0.83**8521	**−0.8393**17	**−0.83932**5	**−0.839325**	**−0.839325**
H	0.380665	**0.419**406	**0.4198**07	**0.419812**	**0.419812**	**0.419812**
H	0.380680	**0.419**115	**0.4195**09	**0.419513**	**0.419513**	**0.419513**

[a] The numbers that do not change are shown in bold; atoms involved in hydrogen bonding are also shown in bold.

Hydrogen Bond Accepting Heavy Atoms. The induced charges on the hydrogen bond accepting oxygen and nitrogen atoms given in Table 3 generally increase in line with the quantum mechanical charges. The increased polarity in the water and methanol trimers over the water and methanol dimers (respectively) is well reproduced as is the increase in polarity for the water formaldehyde heterotrimer over the corresponding dimer. There is a greater tendency to overestimate the charges in hydrogen bond accepting oxygen atoms compared to the hydrogen bond donating oxygen atoms; this is partly due to the inherent deficiencies of the point charge approximation and partly due to the method of distributing an induced dipole over neighboring centers. However, the comparatively larger increase in polarity of O^4 in U and T is well reproduced.

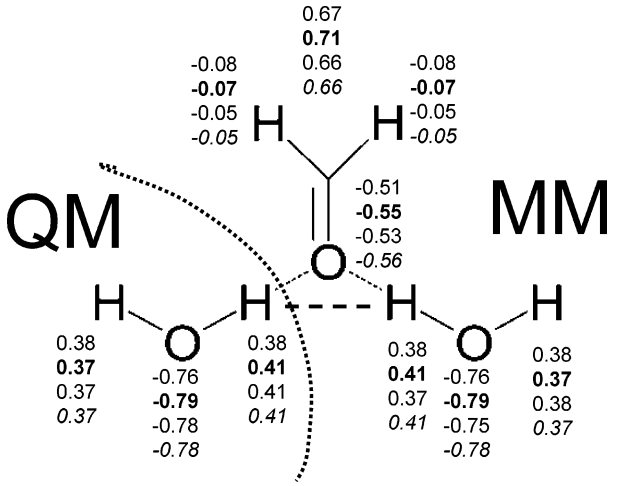

Figure 3. Repulsive H−H interaction that can give rise to anomalous induced charges unless the classical correction is applied. The order of the charges is as follows. Top row monomer, second row full QM (bold), third row no classical correction, fourth row with classical correction. For the quantum part (denoted QM), all charges are QM charges; For the classical part (denoted MM) only first 2 rows are QM charges. All charges are fully converged, i.e., after 4 iterations.

Hydrogen Bond Donating and Accepting Heavy Atoms. The increase in the charge on the atoms in Table 4 that accept as well as donate hydrogen bonds is greater than their counterparts in Tables 2 and 3, and this increase is reproduced well by the induced charges. The polarization effects in the cyclic systems appear to be more additive than in the acyclic systems according to the QM calculations but not according to the QM/MM calculations. However, the greater polarity in the cyclic systems may be supplemented by greater basis set superposition effects—the counterpoise correction is certainly larger for the cyclic systems (3.8 kJ mol^{-1} compared to 3.2 kJ mol^{-1} for the cooperative water trimer and 5.0 kJ mol^{-1} compared to 3.9 kJ mol^{-1} for the cooperative methanol trimer). Under these circumstances there is probably some uncertainty in the benchmark quantum calculations (despite the use of a large basis set to minimize the basis set superposition error). Nevertheless, the general conclusion to emerge from Tables 2−4 is that the induced charge method gives a good qualitative reproduction of the charge distribution in the MM part of the systems presented in Figures S1−S5.

Importance of the Classical Correction to the Field. Figure 3 shows qualitatively why it is advantageous to include the classical correction to the field for certain configurations. Here a classical formaldehyde accepts a hydrogen bond from the quantum water (and the classical water). Though the classical water does not donate a traditional hydrogen bond to the quantum water as the distance is too great, it still presents a hydrogen toward the quantum hydrogen. The polarizing effects of the quantum water minimize this mildly repulsive H···H interaction by reducing the charge on the classical hydrogen from 0.38 to 0.37 (third row in Figure 3); there is an anomalous decrease in the polarity of the oxygen atom (to −0.75) and an increase in polarity from 0.37 to 0.38 for the other hydrogen. In reality, the hydrogen bond with the classical formaldehyde should result in increased polarity. This effect can be incorporated via the classical correction to the field and here this results in an increase in charge on the hydrogen from 0.38 to 0.41 (fourth row in Figure 3), which agrees with the full quantum mechanical calculations. For this reason, all of the results in Tables 2−4 included the classical correction.

TABLE 6: Regression Analysis, $Y = mx$, Where y Is the B3LYP Atomic Charges from the Full QM Calculations and x Is the Approximation to This[a]

row	system	N	it. no.	class. corr	R^2	std dev	F	m	δm	t
1	monomer	33			0.998	0.032	13890	1.096	0.009	118
2	*QM*/MM	33	0	−	0.999	0.019	37663	1.009	0.005	194
3	*QM*/MM	33	1	×	0.999	0.021	32073	0.997	0.006	179
4	*QM*/MM	33	4	×	0.999	0.021	31915	0.997	0.006	179
5	*QM*/MM	33	1	√	0.999	0.020	34588	0.994	0.005	186
6	*QM*/MM	33	4	√	0.999	0.020	34804	0.992	0.005	187
7	QM/*MM*	66	1	×	0.997	0.033	27505	1.021	0.006	166
8	QM/*MM*	66	4	×	0.997	0.032	26877	1.019	0.006	164
9	QM/*MM*	66	1	√	0.999	0.025	45145	0.975	0.005	212
10	QM/*MM*	66	4	√	0.998	0.026	41125	0.964	0.005	203

[a] The simplest approximation is the monomer charges. Where x is the quantum charges in QM/MM systems, they are denoted *QM*/MM, whereas the induced charges are denoted QM/*MM*. The classical correction ("class. corr") to the field is defined in the methods section. The number of compounds and the number of iterations of the induced charges ("it. no.") is also given.

Effect of the Induced Charges on the QM System. The effect of classical polarization in the MM entity on the atomic charges that can be calculated for the QM entity using mulfit is less marked as they are already polarized through the SCF process and so the additional polarization is small. In Figure 3 there is no effect visible at 2d.p. in the charge on the quantum oxygen atom, and a small increase of 0.1 in the charge of the quantum hydrogen that donates a hydrogen bond (regardless of whether the classical correction is included or omitted). The effect of MM polarization in improving the QM atomic charges can be detected by regression analysis of the charges, as shown in Table 6, but the effect on the energetics of interaction is more noticeable because this involves both the QM and MM atoms.

Regression Analysis of the Induced and Quantum Charges. Using atomic charges from the full QM calculations as a benchmark, regression analysis has been used to assess whether MM polarization improved charges on the key atoms involved in the trimer interactions, as discussed above, for both the QM entity and the MM entity. For the acyclic water trimers, these key atoms are the central OHOHO atoms that form the linear H-bond arrangement; for the cyclic trimers the key atoms are the ring of 3 OH groups. Carbonyl carbons are also included as key atoms. The results are given in Table 6. Trimer formation results in polarization of the monomers, and this is reflected in the regression coefficient, m, taking a value greater than 1.0—the value of ∼1.1 (row 1, Table 6) suggests an increase in polarity of ∼10%. The QM/MM charges in the QM entity correlate much better with the QM charges: the coefficient drops from ∼1.1 to ∼1.01 (row 2), which is much nearer the ideal value of 1.0, even without MM polarization. One iteration of polarization of the MM charges takes m to a value of 0.997 (row 3), which is even closer to the ideal value but subsequent iteration does not result in more improvement of the QM charges (row 4). If the classical correction is applied to the polarized MM charges, m for the QM charges drops marginally to 0.994 (row 5, 1 iteration) but the F value increases. Subsequent iteration (row 6) improves F and t marginally but also reduces m marginally.

Similar improvements are seen in the MM charges. One iteration in the absence of the classical correction sees m drop from ∼1.1 (row 1, monomer charges) to ∼1.02 (rows 7 and 8), which again is nearer to the ideal value of 1.0. Application of the classical correction sees m drop from ∼1.1 to 0.98 (row 9), giving a similar improvement in m, but this is accompanied by a more notable increase in F and t. The results after one iteration

TABLE 7: Standard Statistical Descriptors for Regression Analysis on Hartree−Fock (HF) and B3LYP QM/MM Dimer Interaction Energies Using the Equation $E_p = mE_{method}$, where E_p is the Energy Calculated Assuming "Perfect Polarization" (i.e., Using Charges Derived from the Full QM Calculations) and E_{method} is One of the Methods below, i.e. with 0, 1 or 4 Iterations

	HF method			B3LYP method		
	0 iterations	1 iteration	4 iterations	0 iterations	1 iterations	4 iterations
R^2	0.999	1.000	1.000	0.999	1.000	1.000
std dev	1.86	0.99	0.95	1.81	0.94	0.91
F	6162	21716	23568	6023	22309	23839
m	1.104	0.983	0.976	1.106	0.985	0.978
δm	0.014	0.007	0.006	0.014	0.007	0.006
t	79	148	154	78	149	154

(row 9) are superior to those after 4 iterations (row 10). However, it should be noted that although the visual analysis in Tables 2−4 and the regression analysis in Table 6 provides evidence that the atomic charges are polarizing in a meaningful way, perfect agreement with the quantum mechanical charges cannot be expected for two reasons. First, it is well-known that atomic charges are not rigorously defined within quantum mechanics. Second, the partitioning of an induced dipole at an atomic center onto the neighboring centers inevitably means that the regression cannot be perfect, and this is the reason m tends to move further away from 1.0 on subsequent iteration. For this reason, the true test of the method is not how well it reproduces changes in the atomic charges, though this can be useful for gaining chemical insight, but how well it reproduces the energetics.

Electrostatic and Polarization Energies. The atomic charges determined by the full QM calculations can be taken to represent the "definitive" result that would occur if the polarization process worked perfectly. Clearly the phrase "definitive" needs to be used with caution, as basis set superposition effects are not zero despite the use of a large basis set, but is clearly reasonable to set these calculations as the benchmark for QM/MM calculations performed with the same functional. The B3LYP electrostatic and polarization energies resulting from this process are compared to those determined with no MM polarization and those determined using MM polarization, with and without iteration for the dimeric systems in Figure 4. Despite the inherent polarity of Hartree−Fock wave functions, Table 7 shows that the regression analysis for the B3LYP energies in Figure 4 and the corresponding Hartree−Fock energies (not shown) are essentially identical. Here we merely note that the marked polarity of Hartree−Fock wave functions with small basis sets is much less marked for large basis sets and this is probably the origin of this equivalence. For this reason, the corresponding Hartree−Fock results for the trimer systems with and without the classical correction are shown in Figure 5. The results in Figures 4 and 5 and Table 7 clearly show that the QM/MM electrostatic and polarization energies with no MM polarization underestimate the "definitive" energies by about 9−12% (as judged by the slope of the best-fit lines, which is ∼1.105). With MM polarization and four cycles of iteration, the dimer electrostatic and polarization interaction energy is overestimated by about 2.3%, or 1.6% with just one iteration (the slopes are ∼0.977 and 0.984, respectively). The results for 1 iteration are not shown in Figure 5 as the line is too close to the line for 4 iterations. Because the results with and without iteration are essentially equivalent, there is little to be gained by iteration and indeed the results without iteration are actually slightly superior as well as taking just 40% of the time. For the trimer systems without the classical correction, the interaction energy is underestimated by about 2.9%, but with the classical correction the error decreases to a slight 0.8% overestimate. In contrast to the QM/MM interaction energies without MM polarization, all four MM polarization schemes in Figures 4 and 5 give rise to correlations that lie close to the 45° degree ideal line. It would seem reasonable to conclude that only one iteration is required and that the classical correction is desirable but not essential. Indeed, in a similar implementation of this approach designed for molecular dynamics simulations,[43] we note the liquid water oxygen−oxygen radial distribution function was well-reproduced without iteration.

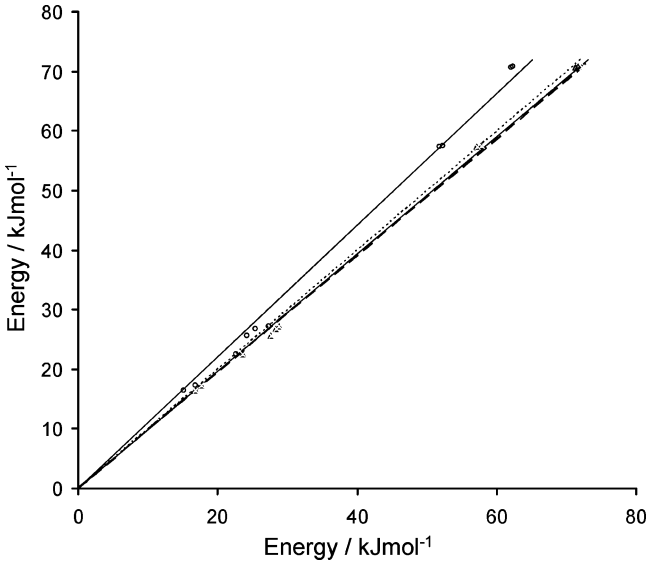

Figure 4. Relationship between the B3LYP QM/MM electrostatic plus polarization dimer interaction energy determined using "perfect" polarization and that determined using polarization modeled using induced charges. The line for equality between the two methods is indicated by short dashes. The results for QM/MM with no MM polarization lie above the ideal line and are indicated by squares and a solid line. The results for one iteration of MM polarization lie slightly below the ideal line and are indicated by triangles and a solid line. The results for four iterations of MM polarization lie slightly further below the ideal line and are indicated by crosses (which are generally obscured by the triangles) and long gray dashes.

Comparison against Morokuma Energy Decomposition Analysis. A comparison of the QM/MM polarization energy with that calculated for the dimers using Morokuma energy decomposition analysis is given in Figure 6 (optimized geometry) and Figure S6 (optimized geometry extended by 1 Å). The molecules are indicated on the x axis. Several general trends that emerge from these calculations can be seen by analyzing the results for the fully optimized water dimer denoted WW (Figure 1a and Figure 7a). First, the QM/MM polarization energies are in good agreement with the Morokuma energy decomposition analysis—indeed in all cases in Figure 6 and Figure S6 the agreement is within the error bars and is usually well within the error bars. Second, there is a difference between the QM + MM and the MM + QM results; the superior results are obtained when the H-bond donating water of Figure 1 is

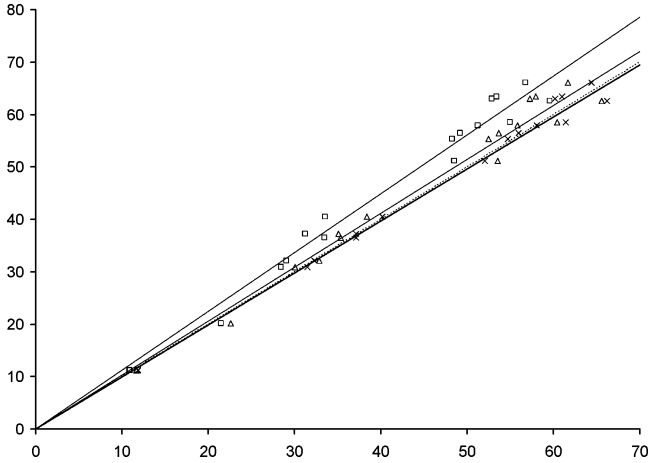

Figure 5. Relationship between the HF QM/MM electrostatic plus polarization trimer interaction energy determined using "perfect" polarization and that determined using polarization modeled using induced charges. The results for QM/MM with no MM polarization lie well above the ideal line (short dashes) and are indicated by squares and a solid line. The results for QM/MM with full MM polarization (4 iterations) but no classical correction lie slightly above the ideal line (short dashes) and are indicated by triangles and a solid line. The results for QM/MM with full MM polarization (4 iterations) and classical correction lie just below the ideal line (short dashes) and are indicated by crosses and a solid line.

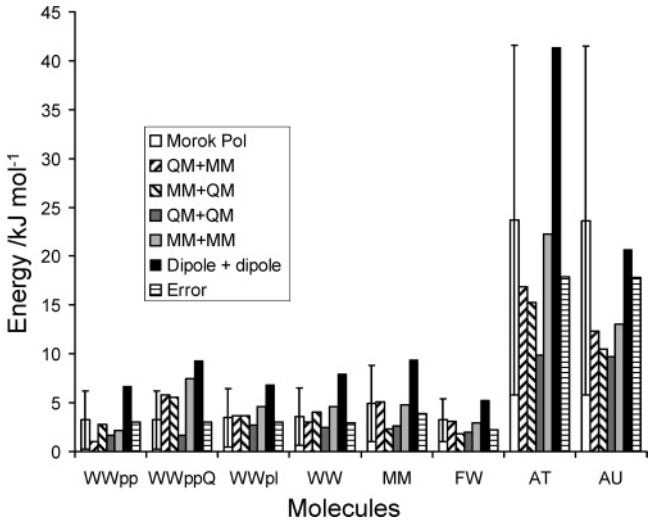

Figure 6. Polarization energy calculated using Morokuma energy decomposition analysis, QM/MM methods and classical methods. W denotes a water molecule, F denotes formaldehyde, M denotes methanol, A denotes adenine, T denotes thymine, and U denotes uracil. Perpendicular attack of water in the WW dimer is denoted pp, ppQ denotes addition of off-atom point charges and pl denotes a completely planar system. The order of the bars is given in the key: Morok Pol denotes polarization from Morokuma energy decomposition, QM + MM denotes that the polarization energy is the sum of the SCF polarization energy for monomer A plus the MM polarization energy for monomer B. MM + QM denotes that the polarization energy is the sum of the SCF polarization energy for monomer B plus the MM polarization energy for monomer A. QM + QM denotes the sum of the SCF polarization energies for monomers A and B; MM + MM denotes the sum of the MM polarization energies for monomers A and B. Dipole + dipole is the traditional polarization energy calculated from the induced dipoles for both A and B. Error is the sum of the mix term and the counterpoise correction and is used to set the error bars on the polarization energy calculated using Morokuma energy decomposition analysis.

the QM entity. Third, the combined QM polarization energies inevitably underestimate the effect, because in the QM/MM calculation of E_3, the MM part is not at all polarized and so the

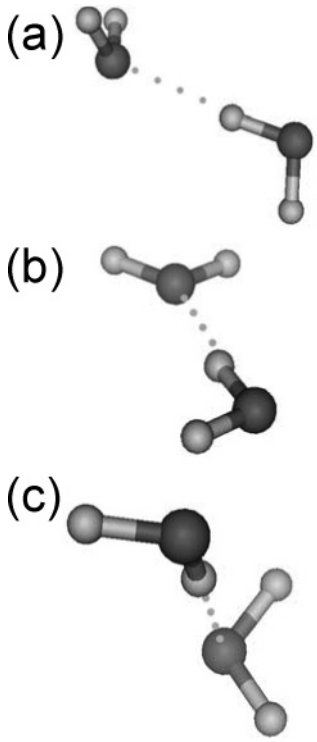

Figure 7. Water dimer orientations used for the Morokuma energy decomposition analysis. (a) WW, the fully optimized geometry as in Figure 1a. (b) QQpl, as in (a) but constrained to be planar. (c) QQpp, the H-bond donating group was constrained to approach perpendicular to the plane of the second water at an intermolecular distance equivalent to that in (a).

QM part is also not fully polarized. For the same reason, the combined MM polarization energies slightly overestimate the effect. The induced dipole approximation greatly overestimates the effect, but unlike the overestimation in the combined MM polarization energies, this is not due to an arbitrary partitioning. In a previous article on induced charges, we regarded the induced dipole approximation as a superior model and assessed the induced charge model by how well it reproduced the induced dipole polarization energies.[43] Generally, the induced charge model reproduced a fraction of the polarization energy, which in most orientations was adequate but was low for a water dimer where the second water approached from a direction perpendicular to the HOH plane (as in Figure 7c). Figures 6 and S6 suggests that the induced charge model may actually be superior to the induced dipole model, which does not always agree to within the error bars of the Morokuma energy decomposition analysis. The induced dipole model is inherently isotropic whereas the induced charge model is inherently anisotropic as it is constrained by the molecular structure.

For the water dimer of Figure 1 (WW), the classical water model cannot polarize perpendicular to the plane. We therefore see superior results in the planar WWpl system (Figure 7b) where this deficiency is artificially removed. In cases such as WWpp (Figure 7c) where there should be significant polarization perpendicular to the plane, Figure 6 (second bar) shows that this anisotropic model underestimates the polarization energy. However, the isotropic model (sixth bar) overestimates the polarization by a greater amount and so is in greater error. Indeed, the anisotropic induced charge model is superior to the isotropic induced dipole model in all the systems represented in Figures 6 and S6.

The problem of polarization perpendicular to the plane can be addressed using point charges sited 0.1 Å above and below

TABLE 8: B3LYP/DZVP QM/MM Interaction Energies (kJ mol^{-1}) between Methylsuccinyl-Ala-Ala-Pro-Ala Chlormethyl Ketone and Various Selected Human Neutrofil Elastase Residues[a]

atom/residue	R/Å	X(QM)	elec $E_2 - E_1$	SCF pol $E_3 - E_2$	MM pol $(E_4 - E_3)/2$	MM pol $(E_5 - E_4)/2$	total polarization
O V31	10.9	H Alm 5	−0.33	−0.06	0.00	0.00	−0.06
HηY94	4.1	2HB Pro 4	0.85	−0.06	−0.01	0.00	−0.07
Hδ2 F192	2.1	HA Alm 5	−10.82	−0.91	−0.83	−0.02	−1.76
H G193	1.9	O Alm 5	−12.37	−1.70	−1.73	−0.07	−3.50
Hγ S195	2.1	HXT Alm 5	5.37	−1.74	−0.34	−0.00	−2.09
O V216	2.0	H Ala 3	−26.09	−3.07	−2.55	−0.19	−5.81
H G218	2.3	HO1 MSU1	−0.73	−0.61	−0.56	−0.09	−1.09

[a] The closest distance of approach, R, between key atoms is also given along with the identity of these residues, which can also be found by reference to Figure 8. "Elec" is the electrostatic interaction energy ($E_2 - E_1$), "SCF pol" is the polarization energy due to the SCF process ($E_3 - E_2$), "MM pol" is the polarization energy due to the induced charges from ($E_4 - E_3$) or ($E_5 - E_4$), and "total" is the sum of the SCF and MM polarization energies. The classical correction to the field was not applied.

the plane, as shown in Figure 6 (WWppQ). However, the polarization energy is overestimated and the resulting induced charges (not shown) are nonphysical. We therefore conclude that although the methodology permits such an approach, it would require a degree of parametrization that is beyond the scope of this article.

The polarization energy component of the energy relative to the total electrostatic and polarization energy in Figures 4 and 5 is 15 ± 3% for 1 iteration or 15 ± 4% for full iteration. This percentage is remarkably close to the 14 ± 5% for the (different) systems in Figure 6. (The percentage relative to the total quantum mechanical interaction energy is much higher (37 ± 19%) because the exchange repulsion term is almost equal and opposite in magnitude to the electrostatic term; the polarization term is similar in magnitude to the charge-transfer term.) This percentage drops to 6 ± 2% for the systems extended by 1 Å (Figure S6) where the equilibrium bond length has been extended by 1 Å (and the percentage relative to the total energy is similar at 6 ± 2% because the exchange-repulsion term is reduced significantly in magnitude). Consideration of these values shows that although polarization is not the most important term, its magnitude is sufficiently large to determine the outcome of competing reactions with similar energetics. These calculations show that the SCF polarization is less than half of the full polarization energy, hence the need for MM polarization.

In summary, we conclude that when assessed against Morokuma energy decomposition analysis, the QM/MM induced charge model performs well.

Contribution to Protein−Ligand Interactions. To assess the affect of geometry on the polarization calculations, we have studied two systems of biological interest. The first is the 1.84 Å structure of human neutrophil elastase, a serine protease interacting with the peptide analogue ligand methylsuccinyl-Ala-Ala-Pro-Ala chlormethyl ketone. Hydrogen atoms were added and the system was minimized using MOE. It therefore represents an equilibrium system before attack on the Ala P1 carbonyl group by Oγ of Ser 195 (The key C−O distance is 3.24 Å). The second system is propranolol (a β-adrenergic antagonist) interacting with a model of the β_2-adrenergic receptor[101] generated from a restrained molecular dynamics study. The energy components for the pair wise interaction between the quantum mechanical ligand and selected classical residues are given in Tables 8 (peptide ligand) and 9 (propranolol).

For the peptide inhibitor (Figure 8, Table 8), the polarization energy can amount to 30% of the electrostatic energy (Gly 193), and for Gly 218 is even greater in magnitude. In this configuration, the polarization energy significantly reduces the repulsive electrostatic interaction between Ser 195 and the inhibitor. In Figures 4 and 5 the polarization energy contributed a much more constant proportion (15 ± 4%) as the systems were all hydrogen bonded. Here the interactions are more heterogeneous and the polarization ceases to be such a uniform proportion and this is probably the main reason for including it.

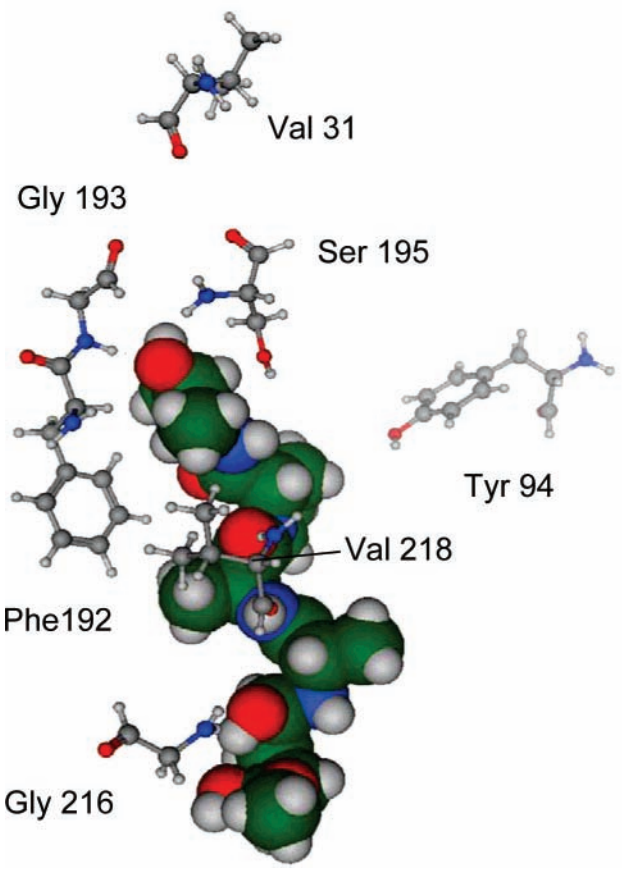

Figure 8. Space-filled peptide analogue ligand methylsuccinyl-Ala-Ala-Pro-Ala chlormethyl ketone interacting with selected residues from human neutrophil elastase.

A similar picture emerges in the propranolol−β_2-adrenergic receptor interaction (Table 9, Figure S7). Here we see that the electrostatic interaction energy can be positive (residues 264, 289, 293) or negative (residues 103, 183, 283), but the SCF procedure always lowers the energy; for residues 103 and 293 this lowering is insignificant because of the long distances involved. For the close interactions, the polarization energy due to the induced charges is generally of the same magnitude as the SCF polarization energy (e.g., for Asn 264), but for Asn 183, this lowering is greater (−1.1 compared to −0.1 kJ mol^{-1}). In all cases apart from Asn 283, the SCF energy converged to 5 decimal places after just one iteration of the polarization

TABLE 9: HF/6-31G* QM/MM Interaction Energies (kJ mol^{-1}) between Propranolol and Various Selected Asparagine Residues[a]

Asn	*R*/Å	X(QM)	X(Asn)	elec $E_2 - E_1$	SCF pol $E_3 - E_2$	total MM pol	total polarization
103	15.2	H($C_{1'}$)	O	−1.9	0	−0.1	−0.1
183	4.3	H($C_{1'}$)	$O_{\delta 1}$	−5.1	−0.1	−1.1	−1.2
264	5.2	H_3	$H_{\delta 21}$	2.4	−0.1	−0.2	−0.3
283	2.3	H($C_{3'}$)	N	−22.7	−1.4	0.3	−1.1
289	2.4	H_8	$H_{\delta 22}$	19.8	−1.0	−0.5	−1.5
293	9.3	H_8	$H_{\beta 3}$	6.4	0.0	−0.1	−0.1

[a] The closest distance of approach, *R*, between key atoms is also given along with the identity of these residues, which can also be found by reference to Figure S7. Here H($C_{1'}$) indicates a hydrogen atom attached to carbon labeled $C_{1'}$. The other details are as for Table 8.

process; in all cases the energy had fully converged after just two iterations. The results for residue 289 (as for Ser 195 above) are illuminating as they show a net gain in polarization energy of −1.5 kJ mol^{-1}, showing that polarization can play a role in helping to reduce repulsive interactions in protein−ligand interactions, as well as further stabilizing attractive interactions. The origin of the anomalous positive polarization energy for Asn 283 (MM pol = 0.3) is similar to that for the anomalous results for $H_2CO{\cdot}2H_2O$ (Figures 2 and S2) when the classical correction was not included and is reported to illustrate that care must to be taken in partitioning the system.

Here we have sought to gain additional insight into the interactions within the β_2-adrenergic receptor−ligand complex by applying the method at a geometry pre-computed using a lower level of theory. Such an approach is well established within theoretical chemistry, as most elegantly illustrated in the various variants of ONIOM,[33,102−104] G1,[105] G2[106] and G3[107] levels of theory. For more detailed applications involving geometry optimization or molecular dynamics, the strategy should be implemented with a variant of the mulfit approach for which derivatives are readily calculated.[43]

Conclusions

We have presented a method for modeling polarization and have assessed its performance in hybrid QM/MM calculations on a number of small molecule systems. The method is based on the induced dipole approach (eq 1) but exploits existing methodology for calculating potential-derived point charges[59,72] from distributed multipole series[74] to express the induced dipoles as a set of "induced" charges on the atom carrying the isotropic polarizability, α, and those bonded to it. The method has the advantage that the same methodology is used to determine the induced charges and the potential derived charges and so both sets of charges are rigorously defined within the same framework. The link with the wave function is therefore retained and this is the origin of the method's distinct compatibility with hybrid QM/MM methods. The advantage of the induced charge approach is that the method is readily interfaced with quantum mechanical methods and has the added advantage that the induced charges are more readily interpreted than induced dipoles.

Regression analysis of the hybrid MM induced charges and the hybrid QM charges against those derived from full quantum mechanical calculations shows that the method works well. This assessment has been supplemented by visual inspection: the ease of interpretation is illustrated by analysis of the charges involved in cooperative and anticooperative hydrogen bonding systems. It is encouraging that polarization effects in water are modeled well and this may be important, not only for modeling water mediated protein−ligand interactions, as observed for example in HIV protease and dihydrofolate reductase, which may require a hybrid QM/MM approach, but also for modeling bulk water where it has been shown that standard water models do not necessarily reproduce the asymmetric strength of hydrogen bonds in bulk water.[108]

Polarization effects generally contribute about 10% of the total energy and so including polarization in the MM region of a hybrid QM/MM calculation makes a significant contribution to the total interaction energy. Thus in the applications reported here, the polarization energy is roughly twice that reported in standard QM/MM calculations with fixed MM charge distributions. The "benchmark" polarization energy calculations show that the use of well-chosen standard unmodified polarizabilities gives good interaction energies.

For the small dimeric systems presented here, implementation of the method is straightforward. For more complex systems, consideration of geometric effects is important in setting up the calculations as two contrasting effects are significant. Though the basic method involves iteration, the results, particularly those involving interactions at nonequilibrium distances or interactions to distant residues within a protein, show that in many cases only one iteration is required. Indeed, many interactions within a protein could be ignored completely because the polarization effects are so small. However, for certain trimers and other more complex systems such as Asn 283 in the receptor:ligand complex, care needs to be taken in partitioning the system so classical-classical polarization is included where necessary.

Supporting Information Available: Figures S1−S7 of atomic charges, polarization energies, and the interaction between propranolol and asparagine residues. This material is available free of charge via the Internet at http://pubs.acs.org.

References and Notes

(1) Mulholland, A. J.; Grant, G. H.; Richards, W. G. *Prot. Eng.* **1993**, *6*, 133−147.
(2) Cunningham, M. A.; Bash, P. A. *Biochimie* **1997**, *79*, 687−689.
(3) Bakowies, D.; Thiel, W. *J. Phys. Chem.* **1996**, *100*, 10580−10594.
(4) Park, H.; Brothers, E. N.; Merz, K. M. *J. Am. Chem. Soc.* **2005**, *127*, 4232−4241.
(5) Hermann, J. C.; Hensen, C.; Ridder, L.; Mulholland, A. J.; Holtje, H. D. *J. Am. Chem. Soc.* **2005**, *127*, 4454−4465.
(6) Guimaraes, C. R. W.; Udier-Blagovic, M.; Jorgensen, W. L. *J. Am. Chem. Soc.* **2005**, *127*, 3577−3588.
(7) Topf, M.; Richards, W. G. *J. Am. Chem. Soc.* **2004**, *126*, 14631−14641.
(8) Marti, S.; Andres, J.; Moliner, V.; Silla, E.; Tunon, I.; Bertran, J. *J. Am. Chem. Soc.* **2004**, *126*, 311−319.
(9) Greatbanks, S. P.; Gready, J. E.; Limaye, A. C.; Rendell, A. P. *J. Comput. Chem.* **2000**, *21*, 788−811.
(10) Hall, R. J.; Hindle, S. A.; Burton, N. A.; Hillier, I. H. *J. Comput. Chem.* **2000**, *21*, 1433−1441.
(11) Hart, J. C.; Sheppard, D. W.; Hillier, I. H.; Burton, N. A. *Chem. Commun.* **1999**, 79−80.
(12) Marti, S.; Andres, J.; Moliner, V.; Silla, E.; Tunon, I.; Bertran, J.; Field, M. J. *J. Am. Chem. Soc.* **2001**, *123*, 1709−1712.
(13) Marti, S.; Andres, J.; Moliner, V.; Silla, E.; Tunon, I.; Bertran, J. *Theor. Chem. Acc.* **2001**, *105*, 207−212.
(14) Ridder, L.; Mulholland, A. J.; Rietjens, I. M. C. M.; Vervoort, J. *J. Am. Chem. Soc.* **2000**, *122*, 8728−8738.
(15) Mulholland, A. J.; Richards, W. G. *J. Phys. Chem. B* **1998**, *102*, 6635−6646.
(16) Strajbl, M.; Florian, J.; Warshel, A. *Int. J. Quantum Chem.* **2000**, *77*, 44−53.
(17) Turner, A. J.; Moliner, V.; Williams, I. H. *Phys. Chem. Chem. Phys* **1999**, *1*, 1323−1331.
(18) Varnai, P.; Richards, W. G.; Lyne, P. D. *Proteins* **1999**, *37*, 218−227.
(19) Houjou, H.; Inoue, Y.; Sakurai, M. *J. Phys. Chem. B* **2001**, *105*, 867−879.
(20) Thompson, M. A.; Schenter, G. K. *J. Phys. Chem.* **1995**, *99*, 6374−6386.

(21) Cornell, W. D.; Cieplak, P.; Bayly, C. I.; Gould, I. R.; Merz, K. M.; Ferguson, D. M.; Spellmeyer, D. C.; Fox, T.; Caldwell, J. W.; Kollman, P. A. *J. Am. Chem. Soc.* **1996**, *118*, 2309.

(22) Cornell, W. D.; Cieplak, P.; Bayly, C. I.; Gould, I. R.; Merz, K. M.; Ferguson, D. M.; Spellmeyer, D. C.; Fox, T.; Caldwell, J. W.; Kollman, P. A. *J. Am. Chem. Soc.* **1995**, *117*, 5179−5197.

(23) Weiner, S. J.; Kollman, P. A.; Nguyen, D. T.; Case, D. A. *J. Comput. Chem.* **1986**, *7*, 230−252.

(24) Weiner, S. J.; Kollman, P. A.; Case, D. A.; Singh, U. C.; Ghio, C.; Alagona, G.; Profeta, S.; Weiner, P. *J. Am. Chem. Soc.* **1984**, *106*, 765−784.

(25) Jorgensen, W. L.; Tirado-Rives, J. *J. Am. Chem. Soc.* **1988**, *110*, 1666−1671.

(26) Jorgensen, W. L. *J. Phys. Chem.* **1986**, *90*, 1276−1284.

(27) Jorgensen, W. L.; Swenson, C. J. *J. Am. Chem. Soc.* **1985**, *107*, 569−578.

(28) Jorgensen, W. L.; Madura, J. D.; Swenson, C. J. *J. Am. Chem. Soc.* **1984**, *106*, 6638−6646.

(29) MacKerell, A. D.; Bashford, D.; Bellott, M.; Dunbrack, R. L.; Evanseck, J. D.; Field, M. J.; Fischer, S.; Gao, J.; Guo, H.; Ha, S.; Joseph-McCarthy, D.; Kuchnir, L.; Kuczera, K.; Lau, F. T. K.; Mattos, C.; Michnick, S.; Ngo, T.; Nguyen, D. T.; Prodhom, B.; Reiher, W. E.; Roux, B.; Schlenkrich, M.; Smith, J. C.; Stote, R.; Straub, J.; Watanabe, M.; Wiorkiewicz-Kuczera, J.; Yin, D.; Karplus, M. *J. Phys. Chem. B* **1998**, *102*, 3586−3616.

(30) MacKerell, A. D.; Wiorkiewiczkuczera, J.; Karplus, M. *J. Am. Chem. Soc.* **1995**, *117*, 11946−11975.

(31) Brooks, B. R.; Bruccoleri, R. E.; Olafson, B. D.; States, D. J.; Swaminathan, S.; Karplus, M. *J. Comput. Chem.* **1983**, *4*, 187−217.

(32) Khoroshun, D. V.; Musaev, D. G.; Morokuma, K. *Organometallics* **1999**, *18*, 5653−5660.

(33) Svensson, M.; Humbel, S.; Froese, R. D. J.; Matsubara, T.; Sieber, S.; Morokuma, K. *J. Phys. Chem.* **1996**, *100*, 19357−19363.

(34) Matsubara, T.; Maseras, F.; Koga, N.; Morokuma, K. *J. Phys. Chem.* **1996**, *100*, 2573−2580.

(35) Cox, S. R.; Williams, D. E. *J. Comput. Chem.* **1981**, *2*, 304−323.

(36) Henchman, R. H.; Essex, J. W. *J. Comput. Chem.* **1999**, *20*, 483−498.

(37) Stone, A. J. *Mol. Phys.* **1985**, *56*, 1065−1082.

(38) Fowler, P. W.; Stone, A. J. *J. Phys. Chem.* **1987**, *91*, 509−511.

(39) Buckingham, A. D.; Fowler, P. W.; Stone, A. J. *Int. Rev. Phys. Chem.* **1986**, *5*, 107−114.

(40) Gooding, S. R.; Winn, P. J.; Maurer, R. I.; Ferenczy, G. G.; Miller, J. R.; Harris, J. E.; Griffiths, D. V.; Reynolds, C. A. *J. Comput. Chem.* **2000**, *21*, 478−482.

(41) Winn, P. J.; Ferenczy, G. G.; Reynolds, C. A. *J. Comput. Chem.* **1999**, *20*, 704−712.

(42) Miller, K. J.; Savchik, J. A. *J. Am. Chem. Soc.* **1979**, *101*, 7206.

(43) Ferenczy, G. G.; Reynolds, C. A. *J. Phys. Chem. A* **2001**, *105*, 11470−11479.

(44) Straatsma, T. P.; McCammon, J. A. *Chem. Phys. Lett.* **1990**, *167*, 252−254.

(45) Straatsma, T. P.; McCammon, J. A. *J. Mol. Simul.* **1990**, *5*, 181.

(46) Wang, J.; Jordan, P. C. *J. Chem. Phys.* **1990**, *93*, 2762−2768.

(47) Berendsen, H. J. C.; Grigera, J. R.; Straatsma, T. P. *J. Phys. Chem.* **1987**, *91*, 6269−6271.

(48) Ramnarayan, K.; Rao, B. G.; Singh, U. C. *J. Chem. Phys.* **1990**, *92*, 7057−7067.

(49) Ahlstrom, P.; Wallqvist, A.; Engstrom, S.; Jonsson, B. *Mol. Phys.***1989**, *68*, 563−581.

(50) Sprik, M.; Klein, M. L. *J. Chem. Phys.* **1988**, *89*, 7556−7560.

(51) Caldwell, J.; Dang, L. X.; Kollman, P. A. *J. Am. Chem. Soc.* **1990**, *112*, 9144−9147.

(52) Dang, L. X.; Rice, J. E.; Caldwell, J.; Kollman, P. A. *J. Am. Chem. Soc.* **1991**, *113*, 2481−2486.

(53) Hemmingsen, L.; Amara, P.; Ansoborlo, E.; Field, M. J. *J. Phys. Chem. A* **2000**, *104*, 4095−4101.

(54) Thompson, M. A.; Glendening, E. D.; Feller, D. *J. Phys. Chem.* **1994**, *98*, 10465−10476.

(55) Ferenczy, G. G.; Csonka, G. I.; Náray-Szabó, G.; Ángyán, J. G. *J. Comput. Chem.* **1998**, *19*, 38−50.

(56) Gao, J. L. *J. Comput. Chem.* **1997**, *18*, 1061−1071.

(57) Gao, J. L.; Freindorf, M. *J. Phys. Chem. A* **1997**, *101*, 3182−3188.

(58) Gao, J. L.; Xia, X. F. *Science* **1992**, *258*, 631−635.

(59) Winn, P. J.; Ferenczy, G. G.; Reynolds, C. A. *J. Phys. Chem. A* **1997**, *101*, 5437−5445.

(60) Stern, H. A.; Kaminski, G. A.; Banks, J. L.; Zhou, R. H.; Berne, B. J.; Friesner, R. A. *J. Phys. Chem. B* **1999**, *103*, 4730−4737.

(61) Rick, S. W.; Berne, B. J. *J. Am. Chem. Soc.* **1996**, *118*, 672−679.

(62) Rick, S. W.; Stuart, S. J.; Bader, J. S.; Berne, B. J. *J. Mol. Liq.* **1995**, *65*−*6*, 31−40.

(63) Rick, S. W.; Stuart, S. J.; Berne, B. J. *J. Chem. Phys.* **1994**, *101*, 6141−6156.

(64) Rick, S. W. *J. Chem. Phys.* **2001**, *114*, 2276−2283.

(65) Rappe, A. K.; Goddard, W. A. *J. Phys. Chem.* **1991**, *95*, 3358−3363.

(66) Bret, C.; Field, M. J.; Hemmingsen, L. *Mol. Phys.* **2000**, *98*, 751−763.

(67) Hirshfelder, J. O.; Curtiss, L.; Bird, R. B. *Molecular theory of gases and liquids*; Wiley: New York, 2000.

(68) Field, M. J. *Mol. Phys.* **1997**, *91*, 835−845.

(69) Bryce, R. A.; Vincent, M. A.; Hillier, I. H. *J. Phys. Chem. A* **1999**, *103*, 4094−4100.

(70) Bryce, R. A.; Vincent, M. A.; Malcolm, N. O. J.; Hillier, I. H.; Burton, N. A. *J. Chem. Phys.* **1998**, *109*, 3077−3085.

(71) Ferenczy, G. G.; Winn, P. J.; Reynolds, C. A. *J. Phys. Chem. A* **1997**, *101*, 5446−5455.

(72) Ferenczy, G. G. *J. Comput. Chem.* **1991**, *12*, 913−917.

(73) Stone, A. J.; Alderton, M. *Mol. Phys.* **1985**, *56*, 1047−1064.

(74) Stone, A. J. *Chem. Phys. Lett.* **1981**, *83*, 233−239.

(75) Becke, A. D. *J. Chem. Phys.* **1993**, *98*, 5648−5652.

(76) Hunt, N. T.; Turner, A. R.; Wynne, K. *J. Phys. Chem. B* **2005**, *109*, 19008−19017.

(77) O'Malley, P. J. *J. Phys. Chem. A* **1998**, *102*, 248−253.

(78) Kone, M.; Illien, B.; Graton, J.; Laurence, C. *J. Phys. Chem. A* **2005**, *109*, 11907−11913.

(79) Sosa, C.; Andzelm, J.; Elkin, B. C.; Wimmer, E.; Dobbs, K. D.; Dixon, D. A. *J. Phys. Chem.* **1992**, *96*, 6630−6636.

(80) Godbout, N.; Salahub D. R.; Andzelm, J.; Wimmer, E. *Can. J. Chem.* **1992**, *70*, 560−571.

(81) Boys, S. F.; Bernardi, F. *Mol. Phys.* **1970**, *19*, 553-&.

(82) Kolos, W. *Theor. Chim. Acta* **1979**, *51*, 219−240.

(83) Ferenczy, G. G.; Reynolds, C. A.; Richards, W. G. *J. Comput. Chem.* **1990**, *11*, 159−169.

(84) Carey, C.; Chirlian, L. E.; Francl, M. M.; Gange, D. M. *Glyco-conjugate J.* **1997**, *14*, 501−505.

(85) Stouch, T. R.; Williams, D. E. *J. Comput. Chem.* **1993**, *14*, 858−866.

(86) Bayly, C. I.; Cieplak, P.; Cornell, W. D.; Kollman, P. A. *J. Phys. Chem.* **1993**, *97*, 10269−10280.

(87) Frisch, M. J.; Trucks, G. W.; Schlegel, H. B.; Scuseria, G. E.; Robb, M. A.; Cheeseman, J. R.; Montgomery, J. A., Jr.; Vreven, T.; Kudin, K. N.; Burant, J. C.; Millam, J. M.; Iyengar, S. S.; Tomasi, J.; Barone, V.; Mennucci, B.; Cossi, M.; Scalmani, G.; Rega, N.; Petersson, G. A.; Nakatsuji, H.; Hada, M.; Ehara, M.; Toyota, K.; Fukuda, R.; Hasegawa, J.; Ishida, M.; Nakajima, T.; Honda, Y.; Kitao, O.; Nakai, H.; Klene, M.; Li, X.; Knox, J. E.; Hratchian, H. P.; Cross, J. B.; Bakken, V.; Adamo, C.; Jaramillo, J.; Gomperts, R.; Stratmann, R. E.; Yazyev, O.; Austin, A. J.; Cammi, R.; Pomelli, C.; Ochterski, J. W.; Ayala, P. Y.; Morokuma, K.; Voth, G. A.; Salvador, P.; Dannenberg, J. J.; Zakrzewski, V. G.; Dapprich, S.; Daniels, A. D.; Strain, M. C.; Farkas, O.; Malick, D. K.; Rabuck, A. D.; Raghavachari, K.; Foresman, J. B.; Ortiz, J. V.; Cui, Q.; Baboul, A. G.; Clifford, S.; Cioslowski, J.; Stefanov, B. B.; Liu, G.; Liashenko, A.; Piskorz, P.; Komaromi, I.; Martin, R. L.; Fox, D. J.; Keith, T.; Al-Laham, M. A.; Peng, C. Y.; Nanayakkara, A.; Challacombe, M.; Gill, P. M. W.; Johnson, B.; Chen, W.; Wong, M. W.; Gonzalez, C.; Pople, J. A. *Gaussian 03*, revision C.02; Gaussian, Inc.: Wallingford, CT, 2004.

(88) Stone, A. J.; Dullweber A.; Engkvist, O.; Fraschini, E.; Hodges, M. P.; Meredith, A. W.; Nutt, D. R.; Popelier, P. L. A.; Wales, D. J. 2002 Orient: a program for studying interactions between molecules, version 4.5′. University of Cambridge, 2006; enquiries to A. J. Stone, ajs1@cam.ac.uk.

(89) Henchman, R. H.; Essex, J. W. *J. Comput. Chem.* **1999**, *20*, 499−510.

(90) Cornell, W. D.; Cieplak, P.; Bayly, C. I.; Kollman, P. A. *J. Am. Chem. Soc.* **1993**, *115*, 9620−9631.

(91) Reynolds, C. A.; Ferenczy, G. G.; Richards, W. G. *THEOCHEM* **1992**, *88*, 249−269.

(92) Reynolds, C. A.; Richards, W. G.; Goodford, P. J. *J. Chem. Soc., Perkin 2* **1988**, 551−576.

(93) Reynolds, C. A.; Richards, W. G.; Goodford, P. J. *Anti-Cancer Drug Des.* **1987**, *1*, 291−295.

(94) Holmes, R. E.; Richards, W. G.; Lambros, S. A. *THEOCHEM* **1985**, *22*, 273−279.

(95) Richards, W. G.; Cuthbertson, A. F. *Chem. Commun.* **1984**, 167−168.

(96) Stone, A. J. *J. Chem. Theory Comput.* **2005**, *1*, 1128−1132.

(97) Umeyama, H.; Kitaura, K.; Morokuma, K. *Chem. Phys. Lett.* **1975**, *36*, 11−15.

(98) Schmidt, M. W.; Baldridge, K. K.; Boatz, J. A.; Elbert, S. T.; Gordon, M. S.; Jensen, J. H.; Koseki, S.; Matsunaga, N.; Nguyen, K. A.; Su, S. J.; Windus, T. L.; Dupuis, M.; Montgomery, J. A. *J. Comput. Chem.* **1993**, *14*, 1347−1363.

(99) Petersson, G. A.; Bennett, A.; Tensfeldt, T. G.; Allaham, M. A.; Shirley, W. A.; Mantzaris, J. *J. Chem. Phys.* **1988**, *89*, 2193−2218.

(100) SPSS Inc., 233 S. Wacker Drive, 11th Floor, Chicago, IL 60606, 2006.

(101) Gouldson, P. R.; Kidley, N. J.; Bywater, R. P.; Psaroudakis, G.; Brooks, H. D.; Diaz, C.; Shire, D.; Reynolds, C. A. *Proteins* **2004**, *56*, 67−84.

(102) Maurer, R. I.; Reynolds, C. A. *J. Comput. Chem.* **2004**, *25*, 627−631.

(103) Vreven, T.; Mennucci, B.; da Silva, C. O.; Morokuma, K.; Tomasi, J. *J. Chem. Phys.* **2001**, *115*, 62−72.

(104) Vreven, T.; Morokuma, K. *J. Comput. Chem.* **2000**, *21*, 1419−1432.

(105) Pople, J. A.; Headgordon, M.; Fox, D. J.; Raghavachari, K.; Curtiss, L. A. *J. Chem. Phys.* **1989**, *90*, 5622−5629.

(106) Curtiss, L. A.; Raghavachari, K.; Redfern, P. C.; Pople, J. A. *J. Chem. Phys.* **1997**, *106*, 1063−1079.

(107) Curtiss, L. A.; Raghavachari, K.; Redfern, P. C.; Pople, J. A. *J. Chem. Phys.* **2000**, *112*, 7374−7383.

(108) Wernet, P.; Nordlund, D.; Bergmann, U.; Cavalleri, M.; Odelius, M.; Ogasawara, H.; Naslund, L. A.; Hirsch, T. K.; Ojamae, L.; Glatzel, P.; Pettersson, L. G.; Nilsson, A. *Science* **2004**, *304*, 995−999.

(109) Mulliken, R. S. *J. Chem. Phys.* **1955**, *23*, 1833−1840.